Optical Technologies for Quantum Information Science

Paul Kwiat, Joseph Altepeter, Julio Barreiro, David Branning, Evan Jeffrey, Nicholas Peters, and Aaron VanDevender

Department of Physics, University of Illinois, 1110 W. Green St., Urbana, IL 61801-3080 USA

ABSTRACT

A number of optical technologies remain to be developed and optimized for various applications in quantum information processing, especially quantum communication. We will give an overview of our approach to some of these, including periodic heralded single-photon sources based on spontaneous parametric down-conversion, ultrabright sources of tunable entangled photons, near unit efficiency single- and multi-photon detectors based on an atomic vapor interaction, quantum state transducers based on high efficiency frequency up-conversion, and low-loss optical quantum memories.

Keywords: entanglement, single photon, quantum memory, down-conversion

1. INTRODUCTION

Since its theoretical beginning approximately two decades ago, the field of Quantum Information Science has seen incredible growth in terms of theoretical proposals for quantum computation,[1] cryptography,[2] and metrology,[3,4] as well as experimental implementations of these protocols.[5] Optical systems are extremely well suited to many of these applications, primarily because optical quantum states may be easily prepared, manipulated, and detected with high accuracy, often using only off-the-shelf technologies. Photons are also relatively immune to the deleterious effects of decoherence, compared to other implementations of quantum bits (qubits), and they are a natural choice for the transmission of quantum signals over large distances, as occurs in various quantum communication protocols such as key distribution and teleportation. Moreover, the main disadvantage of photons – that interactions between them are typically far too weak to perform conditional logic, even in the best known nonlinear optical materials – can in principle be overcome using newly discovered methods that exploit the intrinsic nonlinearity of the detection process itself.[6] Assuming the availability of high efficiency photon-counting detectors, reliable single-photon-on-demand sources, and quantum memories, arbitrary quantum gates can be constructed.

In this paper we review some of the optical quantum technologies which we are developing at the University of Illinois at Urbana-Champaign. Among these are: bright and tunable sources of single photons and entangled photons; high-efficiency photon-counting detectors, including the means for detecting infrared telecommunication wavelengths using visible wavelength detectors; and robust, low-loss quantum memories. In addition to their immediate application to various topics in quantum information science, these technologies should have significant benefits for many other practical applications as well, including the areas of metrology and possibly classical communications. In the following section we describe our work on optical sources, including sources of single-photons-on-demand and methods to prepare them in completely arbitrary quantum states; and bright, tunable sources of two-qubit states, including highly (polarization) entangled states, created via the process of spontaneous parametric down-conversion. In Section 3 we discuss the status of current photon detectors, and one scheme for substantially extending their usable wavelength range into the infrared using a novel up-conversion approach. We also describe a theoretical proposal for an in-principle very high efficiency photon-counting system based on cycling transitions in an atomic vapor. In Section 4, we discuss two somewhat related technologies, that of a quantum transducer for converting arbitrary quantum states at one wavelength to another wavelength, and low-loss optical storage systems for the purpose of quantum memory. As nearly all of these projects are works in progress, here we will focus on the underlying concepts and the potential capabilities assuming presently available technology.

E-mail: kwiat@uiuc.edu; phone: (217) 333-9116; fax: (217) 244-7559

2. SOURCES

2.1. Spontaneous parametric down-conversion

Our primary source of photons is the process of spontaneous parametric down-conversion. In this process, a laser pump photon is split into two longer-wavelength daughter photons, historically called the "signal" and "idler" (Fig. 1). The process occurs with small probability (10^{-12} or less) inside a handful of optical materials with nonlinear optical susceptibilities, such as KDP, $LiIO_3$, and BBO. The constraints of energy and momentum conservation, called "phase-matching conditions", allow fine control over the emission modes of the daughter photons, and also lead to entanglements in these degrees of freedom.[7] Entanglement in polarization can also be readily generated.[8,9]

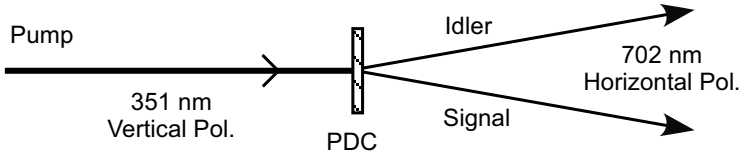

Figure 1. Spontaneous parametric down-conversion (type-I phase matching). A vertically polarized pump photon is annihilated within a nonlinear crystal to create two horizontally polarized "daughter" photons.

2.2. Single-photon source

Because parametric down-conversion (PDC) produces photons in pairs, and does so nonresonantly, it is particularly useful for constructing a single-photon source at visible or telecom wavelengths. (Other possibilities are to use single quantum dots,[10] single impurities,[11] or single atoms[12] as emitters.) By triggering on one of these photons, the other is prepared in a single-photon Fock state.[13] Thus, if only one photon is detected in the idler channel, "heralding" the existence of exactly one signal photon, we let the signal pulse propagate into a storage system, where it waits until released (Fig. 2). If two or more photons are detected in the idler beam, we block the signal pulse. In order to couple well to other systems (e.g., fibers for quantum key distribution, interferometers for all-linear optic quantum computation, atoms for "stored light" or high-efficiency detectors), the mode of the emitted photon is often crucial. The use of down-conversion offers a unique method for controlling this, namely, by restricting the detected mode of the heralding idler photon: Because of the energy and momentum correlations of the photons produced in the down-conversion process, constraining the mode of one of the photons places tight constraints on the mode of the other.[14]

In practice, several problems limit the quality of the single-photon production in terms of the statistics of the (nominally) single-photon emission, efficiency of production, and on-demand delivery of the photons. A typical PDC-based single-photon source includes a pulsed pump laser, a nonlinear crystal where the photon pairs are created, a herald detector where one of the photons is detected, and an optical shutter to suppress photons between heralds; to release the photons "on-demand", one also needs a low-loss switchable optical storage cell.[15] The limitations of each of these components offer opportunities for improvement. First, an optimal source obviously requires high-efficiency conversion of the pump beam into photon pairs. Recent advances in crystal structure engineering permit us to go beyond what has been possible with conventional monolithic crystals. One possibility for improved conversion efficiency is periodically poled lithium niobate (PPLN), both in bulk and in a waveguide structure, allowing for significantly higher nonlinear susceptibilities than are possible with traditional down-conversion crystals.[16,17]

As indicated above, the technique also relies on the capability to reject cases when more than one photon pair is created in a pulse. One solution is to employ photon counters that can distinguish photon number with high quantum efficiency[18] (see Sect. 3). In lieu of such detectors, we can implement multiplexing schemes that allow ordinary "photon-counting" detectors to achieve some of the capabilities of true photon-number detectors; the upper beamsplitter in Fig. 2 is the simplest example, reducing the probability of an undetected double pair by up to a factor of two (for perfect single-photon detection efficiency). The discriminating power of the technique improves by using more spatial (or temporal) modes.[19]

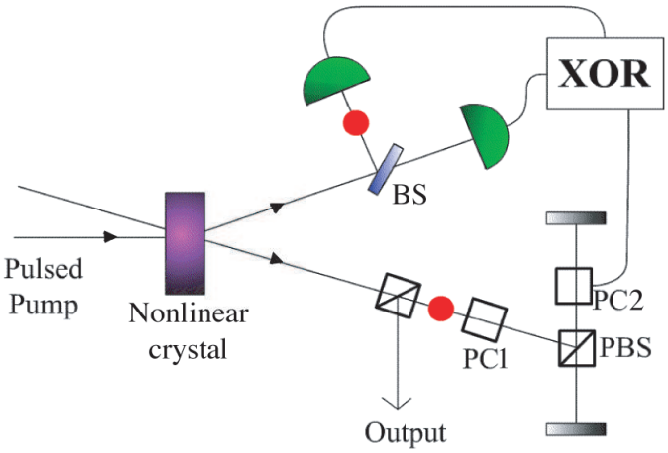

Figure 2. Setup to generate single photons on demand. Photon pairs (represented by the two circles) are generated in the process of spontaneous parametric down-conversion. The signal photon is transferred into the storage cavity only if the trigger system detects exactly one idler photon. By using a series of "weak" pump pulses, the probability of more than one pair per pulse may be kept low while keeping the probability of at least one detected pair from the series of pulses close to one. Also, the 50-50 beam splitter (BS) is meant to represent any multiplexing arrangement to detect any remaining double-pair events. The storage of the signal photon is accomplished by activating Pockels cells PC1 and PC2, which change the signal-photon polarization from horizontal to vertical – so it is reflected by the intra-cavity polarizing beam splitter (PBS) – and back to horizontal (so it remains in the cavity). By reactivating PC2 after the entire series of pulses, the stored photon is released, thereby realizing a periodic source of single photons.

The main innovation of our scheme, however, is to pump the down-conversion crystal with a series of moderate-power pulses, so that there is a high probability that at least one pair will be created in the series, but a low probability that two pairs are created in any particular pulse. By storing the signal photon until a predetermined release time, we can create a periodic source of single photons. The tradeoff is that the final rate of single photons will be somewhat less than the pump rate. Initially we are developing a source with a target single-photon emission rate of ~ 50 kHz. For this purpose we are using a frequency-tripled (1064 nm $\rightarrow$ 355 nm) short-pulsed ($\sim 1/2$ ns) Nd:YAG laser [JDS Uniphase #DNV- 005010-000]. By recycling each ~ 1.2-μJ pump pulse ~ 20 times, we expect a net single-pair probability of 70%, but a net double-pair probability of only 3% *. The latter can be further reduced by using the previously mentioned techniques to detect double-photon events in the idler arm.[19] Finally, one limitation on the single photon probability is loss in the optical storage cavity, primarily in the Pockels cell and polarizing beam splitter. The effects can be mitigated, however, by using a multiple-attempts approach: Even after we store a single photon in the cavity, we keep monitoring the idler arm for another potential single signal photon candidate pulse. If we find one, we switch this into the cavity, simultaneously dumping the (somewhat attenuated) one that had been stored. By transmitting only the most recently stored photon, the effects of loss are minimized. With these techniques, we anticipate a single-photon probability of greater than 90%, with less than a 2% chance of more than one photon.

Assuming this prototype source is successful, we will then investigate the use of a Ti-Sapphire laser to increase the speed to over 1 MHz. Although these rates are lower than those anticipated from some solid state devices, e.g., single quantum dots,[10] this source has greater flexibility in terms of controlling the output spatio-temporal mode, which might be critical, e.g., for applications such as quantum lithography.[3] The other advantage is that the down-conversion sources may be readily modified to emit pairs of maximally entangled photons (i.e., in polarization, or other degrees of freedom – see Sect. 2.4); thus this single-photon source development is a natural step towards the goal of *entanglement* on demand. Finally, by using nondegenerate down-conversion, a telecom wavelength photon may be heralded by an easily detected visible wavelength photon.[20]

*For comparison, the maximum probability for a single photon in an attenuated laser pulse (described by a coherent state) is 37%, with a corresponding 2-photon probability of 18%.

2.3. Arbitrary single-qubit state creation

Central to the long-term future of quantum computing is the capability of performing extremely accurate and reproducible gate operations: the allowable error-per-gate operation should be less than 10^{-4} to 10^{-6} for fault-tolerant operation.[1] Implementing such precise gate operations and preparing the requisite input states is therefore one of the key milestones for quantum information processing. Using optical realizations of qubits, e.g., polarization states of photons, we have the potential to meet these demanding tolerances. Therefore, although large-scale quantum computers will perhaps never be constructed solely using optical qubits, these systems nevertheless form a unique and convenient testbed with which to experimentally investigate the issues surrounding state creation, manipulation, and characterization, and also ways of dealing with decoherence.

As mentioned in Sect. 2.2, when the idler photon from a PDC source is detected, we are left with a good approximation to a single-photon state in the signal beam.[13] We can then apply local unitary transformations to the polarizations of these photons using a birefringent half-waveplate (HWP) and quarter-waveplate (QWP), as indicated in Fig. 3a. We can also controllably introduce decoherence by passing the signal photons through a birefringent delay element. This separates the H and V wavepackets (assuming the eigenaxes of the element

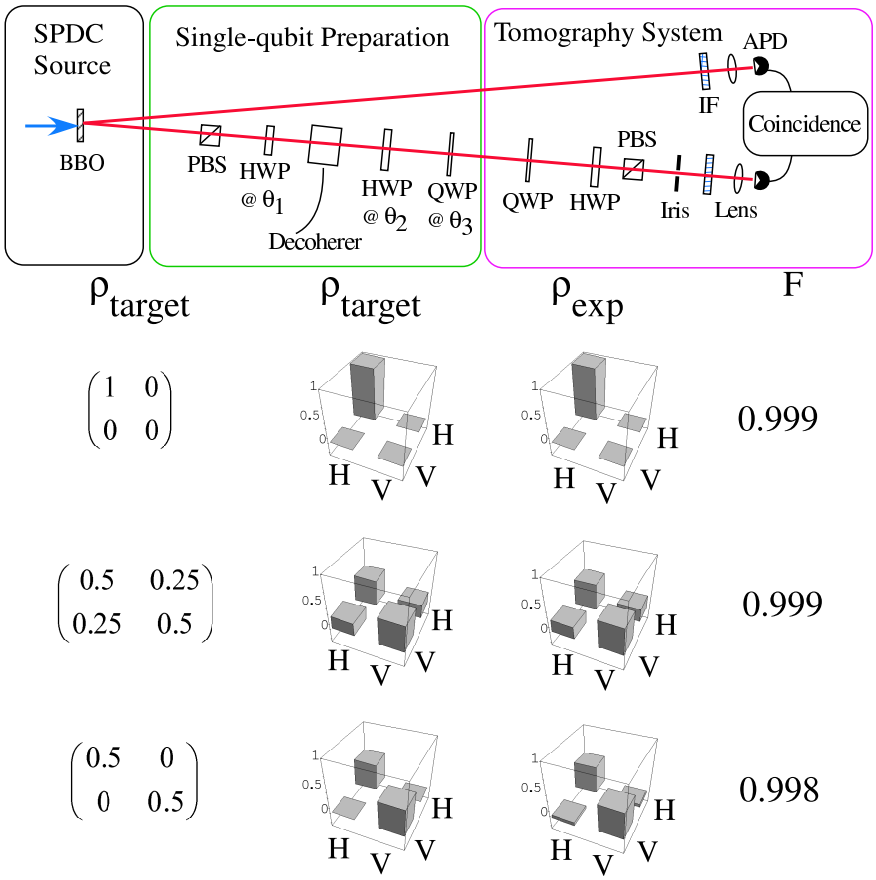

Figure 3. (a) Setup to enable production and characterization of arbitrary single (polarization) qubit states of single photons. The detection of a single photon in the top (idler) arm prepares an approximate single-photon state in the bottom (signal) arm. Waveplates and decohering birefringent elements enable production of arbitrary single-qubit states of the idler photons; these may be characterized with a tomographic measurement of the density matrix, by performing polarization analysis in 3 bases. (b) Typical single-qubit results. On the left are shown the numerical density matrices of the target states, while the second column shows a graphical representation of these. The measured density matrices are shown in the third column; only the real parts are shown, as the imaginary elements are all very small (less than 2%). The final column lists the fidelity between the measured and the target states.

are along H and V) by more than their coherence lengths; the net effect is to entangle the polarization to the frequency. When this extra degree of freedom is traced over (by making a measurement that is insensitive to frequency), the reduced density matrix for the polarization alone will be partially mixed.[21]

Using these techniques for the single photon case, the initial pure horizontal state $|H\rangle$ may be precisely converted into an arbitrary pure or mixed state. We have thereby created a variety of single-qubit states (Fig. 3b). The fidelity [†] of our measured states with our targets is typically greater than 99.8%, and we estimate that we can create and reliably distinguish over 3×10^6 single-qubit states.[23]

2.4. Entangled state creation

Applying the single-qubit techniques of the previous section to *each* output of a down-conversion crystal, we can create arbitrary *product* states for two photons, that is, states with no quantum correlations between the signal and idler polarizations. But these comprise only a very small part of the total two-qubit Hilbert space. To access the rest, we create entangled states by adding a second down-converter with an orthogonal optic axis,[9] as shown in Fig. 4a. Now a given pair of signal and idler photons could have been born in the first crystal, with vertical polarizations, or in the second with horizontal polarizations. These two possibilities cannot be distinguished by any measurements other than polarization, so the quantum state for these photons is a superposition of $|V\rangle|V\rangle$and $|H\rangle|H\rangle$. Because each crystal responds to only one pump polarization, the relative weights of the two down-conversion processes can be controlled by adjusting the input pump polarization. A birefringent phase plate is also added to one of the outputs to control the relative phase of the two contributions, so that we can readily create nonmaximally entangled states of the form[24]

$$|\psi\rangle \propto |H\rangle|H\rangle + \epsilon e^{i\phi}|V\rangle|V\rangle \; . \tag{1}$$

Combined with arbitary single-photon local unitary transformations (implemented using a HWP-QWP-HWP combination), any pure 2-qubit state can be produced. To access states that are not pure, but contain some degree of mixedness, it is necessary to introduce decoherence. This is again accomplished using long birefringent quartz rods, placed in one or both arms [‡]. If the resulting relative timing of the photon detections is in principle sufficient to distinguish the polarization, the reduced density matrix for the polarization alone will be (partially) mixed. With these techniques, we have prepared a variety of two-qubit states.[24, 27, 28] Most recently, we have discovered the necessary ingredients to prepare *arbitrary* states of two qubits, parametrized by 15 independent real numbers.[29]

The density matrices are tomographically determined by measuring the polarization correlations in 16 bases, and performing a maximum-likelihood analysis to find the legitimate density matrix most consistent with the experimental results.[30] In order to improve the speed and accuracy of our tomographic measurements, we have implemented a fully automated system. In addition to reducing the total time for a measurement, and significantly decreasing the uncertainty in the measurement settings, this automated system will also enable the implementation of an adaptive tomography routine – by making an initial fast estimate of the state, most of the data collection time is spent making an optimized set of measurements. With this sort of optimal quantum tomography, we hope to reach the ultimate limit in quantum state characterization.

Our automated system has enabled the creation of a large number of states with widely varying degrees of purity and entanglement. A convenient way to display these states is the "tangle-entropy" plane,[27] shown in Fig. 4b. The tangle is a measure of entanglement: separable states have tangle = 0 while maximally entangled states have tangle = 1. Similarly, pure states have entropy = 0 while completely mixed states have (linear) entropy of 1. Because it is impossible to have a state that is both completely mixed and completely entangled,

[†]The fidelity is a measure of state overlap.[22] For two general density matrices, ρ_1 and ρ_2, the fidelity is $F(\rho_1, \rho_2) \equiv |Tr(\sqrt{\sqrt{\rho_1}\rho_2\sqrt{\rho_1}})|^2$. For two pure states $|\psi_1\rangle$ and $|\psi_2\rangle$, this simplifies to $|\langle\psi_1|\psi_2\rangle|^2$.

[‡]Note that, due to the long coherence length of the parent pump photons, one can now also observe more subtle two-photon interference effects, in which the possibility that the photons were born at one time with one polarization interferes with the possibility that the photons were born at a different time with a different polarization. Consequently, if the photons both experience decoherence in the same basis, then certain states will be completely unaffected. These states comprise a "decoherence-free subspace".[25, 26]

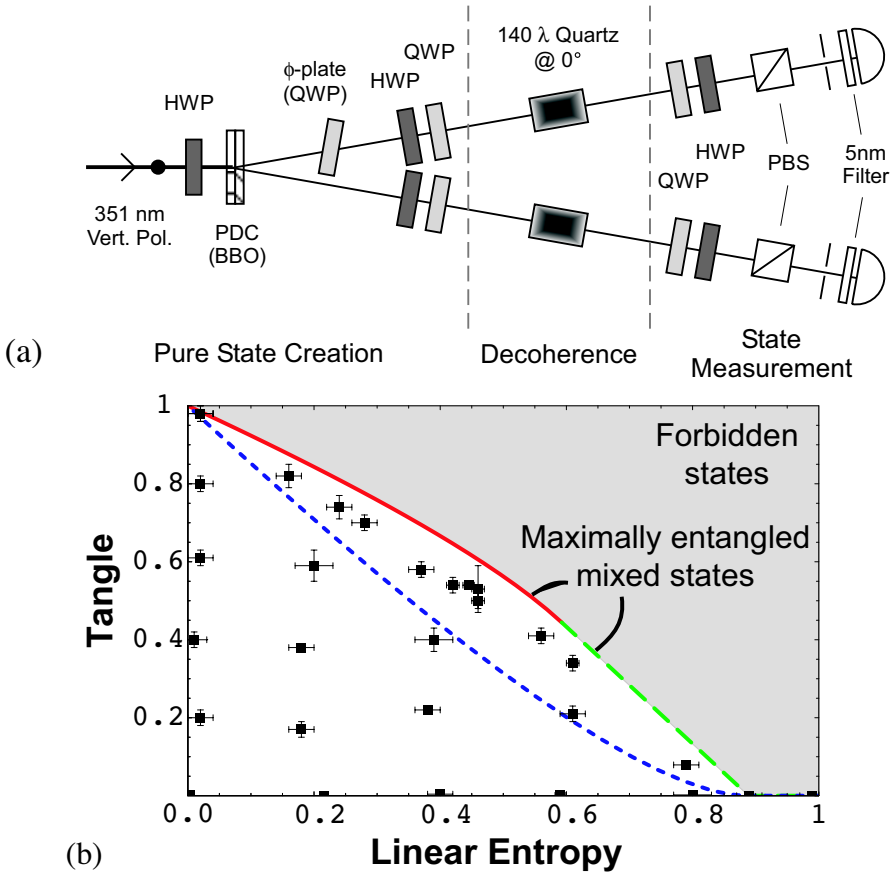

Figure 4. (a) Experimental arrangement for two-photon state creation and verification. A 351-nm laser beam has its polarization adjusted by a half-wave plate (HWP), and generates polarization-entangled photons within a pair of orthogonally oriented PDC crystals. A tipped quarter-wave plate (QWP) in the upper beam adjusts the relative phase between the entangled HH and VV amplitudes, and the polarization of each photon is further individually modified with a HWP and QWP. The photons then pass through decohering elements, consisting of ∼1-cm thick quartz plates. To measure the resultant state, tomography is performed using another QWP, HWP, polarizer (PBS), and detector, that measure the photons' correlations in a total of 16 different bases.[24, 30] (b) The tangle-entropy plane. The upper left corner corresponds to maximally entangled pure states, the lower left corner to pure product states, and the lower right corner to the completely mixed state; states in the upper right portion of the plot are not physically allowed. After their density matrices are determined via tomography, experimentally realized states are plotted here as a function of their mixedness (linear entropy) and their degree of entanglement (tangle). Error bars represent the range of possible tangle-entropy values consistent with the uncertainties in the density matrices. The Maximally Entangled Mixed States (MEMS) lie on the boundary between states that are physically possible, and those that are not. The Werner states (dotted curve) are a class of states once thought to form this boundary.

there is an implied boundary between states that are physically possible and those that are not: this boundary is formed by the "maximally entangled mixed states" (MEMS), which possess the largest degree of entanglement possible for their entropies.[31]

3. DETECTORS

The ability to detect photons with high efficiency and to distinguish the number of photons in a given time interval is a very challenging technical problem with enormous potential pay-offs in quantum communication

and information processing, as well as fundamental physics. For example, violations of Bell's inequalities, which reveal the non-local nature of quantum mechanics, may only be performed indisputably when the detection efficiencies are very high; to date this has not been achieved in any optical experiment. In addition to the obvious relevance for metrology, recent proposals for realizing scalable quantum computing using only linear optics require very high efficiency photon-counting detectors ($> 99\%$).[6,32] In addition, it is crucial that the detectors be able to distinguish the number of incident photons (e.g., tell the difference between 1 and 2 photons, or more generally, between n and $n+1$). Such detectors might also enable the preparation of many-photon entangled states,[33] which could be of great utility in other quantum information schemes, such as quantum lithography. Finally, there are other applications, such as telecom fiber-based quantum cryptography, whose performance is currently limited by poor infrared detector performance.[2,34]

3.1. Current photon detectors

Most modern photon detectors rely to a greater or lesser extent on the photoelectric effect: incident photons are converted to individual photo-electrons, either ionized into vacuum or excited into the conduction band of some semi-conductor. Either way, one is relying on the capability of amplifying single electrons up to detectable levels of current in order to produce a tangible signal For example, the silicon avalanche photodiodes used in many photon counting experiments typically have efficiencies $\eta \approx 75\%$ (though the net *detection* efficiency is usually much less), and rather low dark noise (less than 100 per second).[35] A number of experiments have used a variation of this technology, in which the silicon is lightly doped. These "visible-light photon counters" have displayed efficiencies up to 88%, and predicted to be as high as 95%.[18,35] Moreover, they have demonstrated the ability to distinguish the number of initial photo-electrons produced (which for $\eta \approx 100\%$ is the same as the number of incident photons). Unfortunately, these devices require cooling to 6K, and display very high dark count rates (up to 50,000 s^{-1}), undesirable for quantum communication.

The situation with single-photon detection in the infrared is much worse. Until now, the best means of detecting these photons has been with infrared-optimized APDs, usually InGaAs or Ge. However, these detectors suffer from relatively low quantum efficiency (10%), high dark counts (50,000 – 100,000 s^{-1}) and the need for cryogenic cooling.[36] While efficiencies up to 20% are attainable, the concomitant extra dark count noise reduces the usefulness of these detectors, e.g., for quantum cryptography,[2] where the efficiency limits the bit rate and distance achievable by the key distribution protocol. Thus, any improvements over standard IR APDs would be beneficial for this and other applications.

One possible solution is the use of low temperature superconducting bolometric detectors. These rely on the sudden change in transport impedance at the superconducting transition when a photon is absorbed. Encouraging exploratory work studying these devices has been carried out by several groups.[37,38] Two kinds of devices have been studied. One uses a tungsten film as the sensing element, and operates near 100 mK; because of the low temperature of operation, this device can operate in an energy dispersive mode, both counting the arrival of single photons and obtaining some spectral information.[37] In addition to the inconvenient cryogenic requirement, the time constant of this device is about 10 ms, severely limiting the photon detection rate. In contrast, bolometers made with higher temperature superconductors[38] obtain smaller signals and have not operated in energy dispersive mode, but the detection time constant is significantly shorter, ~100 ps.

3.2. Infrared up-conversion detector

The nonlinear process of frequency up-conversion – the reverse of down-conversion – can greatly enhance single-photon detection in the infrared. After up-converting an infrared photon (at 1550 nm) to a visible one (at 631 nm), we can detect it with silicon APDs, superior to the infrared APDs currently in use.[39] To achieve high-efficiency frequency up-conversion, we use an intense escort laser pulse at 1064 nm (from a pulsed Nd:YAG laser), a very weak input laser, and a bulk crystal of PPLN (see Fig. 5a). The PPLN has been quasi-phase matched to up-convert one photon from the input beam and one photon from the escort beam into a single output photon. Due to energy conservation, the output frequency $\omega_o = \omega_{631}$ is the sum of the input frequency $\omega_i = \omega_{1550}$ and the escort frequency $\omega_e = \omega_{1064}$.

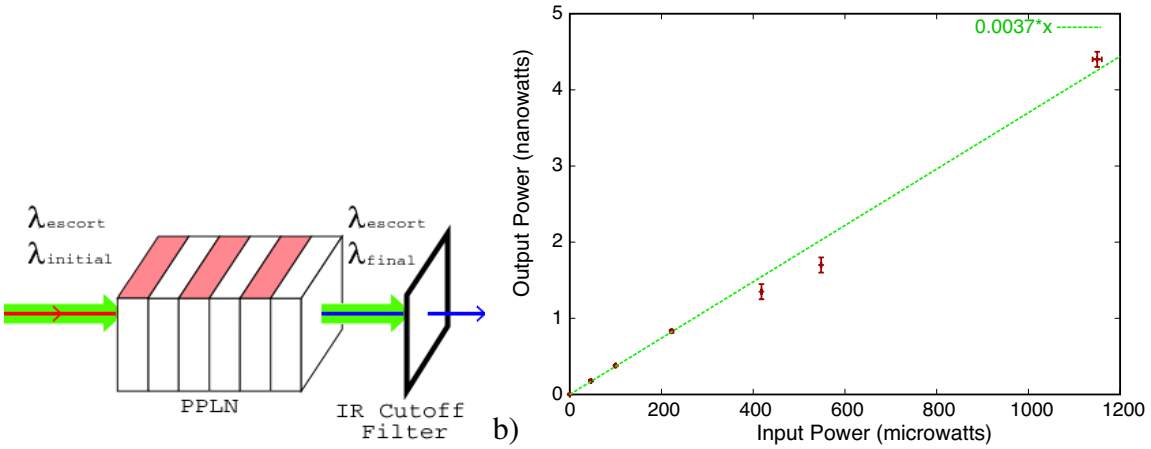

Figure 5. Frequency up-conversion setup and data. (a) Simplified experimental system for high-efficiency detection of IR photons using visible-wavelength detectors. By mixing 1550-nm photons with a strong escort pulse at 1064 nm in a PPLN crystal, it is possible to obtain near unit conversion efficiency to 631-nm photons, which may then be detected by a high-efficiency silicon APD. (b) Experimental plot showing the linear relationship between the output light (632 nm), and the input signal (1550 nm). Although this data was taken with a cw IR signal and a pulsed escort laser at 1064 nm, we can infer an approximate up-conversion efficiency per pulse of $\sim 80\%$.

From the relations that describe the field evolution in a nonlinear medium,[40] we can readily solve for $E_{631}(z)$, the electric field strength of the 631-nm light, as a function of the propagation distance z in the crystal. We find

$$E_{631} \propto \sin\left(\sqrt{\frac{\omega_{1550}\,\omega_{631}}{n_{1550}\,n_{631}}}\,\frac{d_Q E_{1064}}{c}\,z\right), \tag{2}$$

or

$$E_{631} \propto \sin\left(\frac{\pi z}{L_c}\right), \tag{3}$$

where the spatial period L_c for this process is

$$L_c \equiv \sqrt{\frac{\pi^2\,n_{1550}\,n_{631}\,c^2}{\omega_{1550}\,\omega_{631}\,d_Q^2|E_{1064}|^2}}. \tag{4}$$

Here n_{1550} and n_{631} are the $LiNbO_3$ indices of refraction at 1550 nm and 631 nm, respectively, and d_Q is the effective nonlinear coefficient. Because the process is quasi-phase matched we are able to use the largest nonlinear tensor element ($d_{33} \approx 40$ pm/V), more than an order of magnitude larger than the usable element without quasi-phase matching. We note that the evolution of the system is essentially analogous to a Rabi oscillation between the input (1550-nm) and output (631-nm) states, driven by the escort electric field. By choosing a crystal length $L_c/2$, we can achieve very high up-conversion efficiency.

We have measured this up-conversion process in the non-depletion regime, where the output intensity is linear with the input intensity. Figure 5b shows a graph of the output intensity measured using a silicon photodiode at various input intensities. In our experiment the 1064-nm escort beam is pulsed while the 1550-nm input beam is continuous, creating a 631-nm output beam which is also pulsed.[39] The absolute conversion efficiency from input to output is thus very low, since most of the input light passes through the crystal in between escort pulses [§]. However, by knowing the escort intensity profile and the pulse repetition rate (≈ 7.2 kHz), we extrapolate a peak conversion efficiency of greater than 80%. By employing a short *pulsed* 1550-nm source it should be possible to

[§] An alternate approach is being followed by Wong et al., who are using a cw escort beam and a high-finesse power buildup cavity; their reported peak conversion efficiencies are similar to ours.[41]

increase this further, as the photons may then be directed into the crystal when the escort field strength is near its maximum. For a 100-ps signal pulse (compared to the ∼500-ps width of the escort pulse), the calculated conversion efficiency is over 99%. We are in the process of implementing this improvement.

In addition to measuring the up-converted intensity produced by a "classical" input beam, we have also measured high efficiency up-conversion at the single-photon level. By using a series of neutral density filters, we attenuate our 1550-nm source such that, on average, only a single photon overlaps with the escort pulse. By counting 631-nm photons (with a Si APD) in coincidence with the escort pulse, we determined that the efficiency at the single photon level agrees with the 80% value obtained at the higher input intensities. The background during these single photon measurements – defined as the probability of a dark count occuring during a 1-ns window around the photon arrival – was measured to be 3×10^{-4}, mostly due to fluorescence effects from the escort pulse. Further design improvements should reduce this background by another order of magnitude.

3.3. Atomic vapor-based single-photon counting detectors

Finally, we will describe a rather different approach to high-efficiency photon counting.[42,43] Instead of converting each photon to a single photo-electron, we propose a compound process by which a single photon can be converted into many photons. The basis of our proposal is to combine the controlled absorption of light and the high efficiency scheme for projective quantum state measurements in ion traps.[44] Our scheme consists of a cell containing the vapor of some atomic species, e.g., an alkali such as Cesium or Rubidium (Fig. 6). This vapor will be used to coherently absorb the radiation from an incident beam in a controlled fashion. A number of auxiliary lasers prepare the initial quantum state of the atoms in the vapor, and control the interaction of the atoms with the radiation field. The radiation to be detected is directed into the cell along with an "escort" pulse, giving each photon some small probability to excite an atom to a metastable state via a Raman transition. Because there are many atoms, the chance that each photon is absorbed by one of them can be near unity. Next a strong read-out light is applied, which repeatedly excites any atom in the metastable state; the photons resulting from spontaneous decay may then be detected. Because there are many photons produced – typical cycling transition rates are ~ 100 MHz – the chance of not detecting any at all becomes vanishingly small for realistic detector efficiencies. If an imaging photon detection scheme is used, the number of excited atoms may even be counted, thereby allowing one to reliably distinguish input states of different photon number. For a realistic system using 50,000 Cesium atoms cooled to 1 mK, in a cigar-shaped region (2 mm × 100 μm × 100 μm), we estimate a final photon detection efficiency of 99.8%, assuming each photon from the cycling transition is observed with a net efficiency of 10%. However, there remain some serious issues concerning "dark counts" still to be addressed.[45]

4. MISCELLANEOUS

4.1. Quantum state transducer

The capability to faithfully up-convert a single photon in an *arbitrary* polarization state to a higher frequency while preserving the original polarization state is highly desirable, e.g., for distributed quantum computing. The transmission of qubits between quantum computers, especially over large distances, would most easily be accomplished by photons at 1550 nm (which has the highest transmission through fiber optics). Depending on the scheme used for computation, the storage or processing of qubits may likely require photons in the visible spectrum, e.g., corresponding to some atomic transition, and so a method must be developed for converting between wavelengths at the single photon level while coherently maintaining the polarization state.[46]

The single-crystal upconversion scheme described in Sect. 3.2 only operates on one of the polarizations of the incident 1550-nm photon. To faithfully convert an arbitrary polarization state we can incorporate a second PPLN crystal in series with the first, but oriented such that its optic axis is rotated by 90° around the propagation direction (see Fig. 7). By using an escort laser polarized at 45°, i.e., with equal horizontal and vertical components, we can up-convert the horizontal component of the input photon in the first crystal and the vertical component in the second. Note that this is essentially the inverse process of the one discussed in Sect. 2.4 for creating entangled states using two down-conversion crystals.[9] (See also the related work by Shih et al.[47])

After filtering out all of the remaining escort photons, we will be left with a single output photon. Dispersion and birefringence effects in the PPLN crystal will cause the final photon to have an additional phase between its

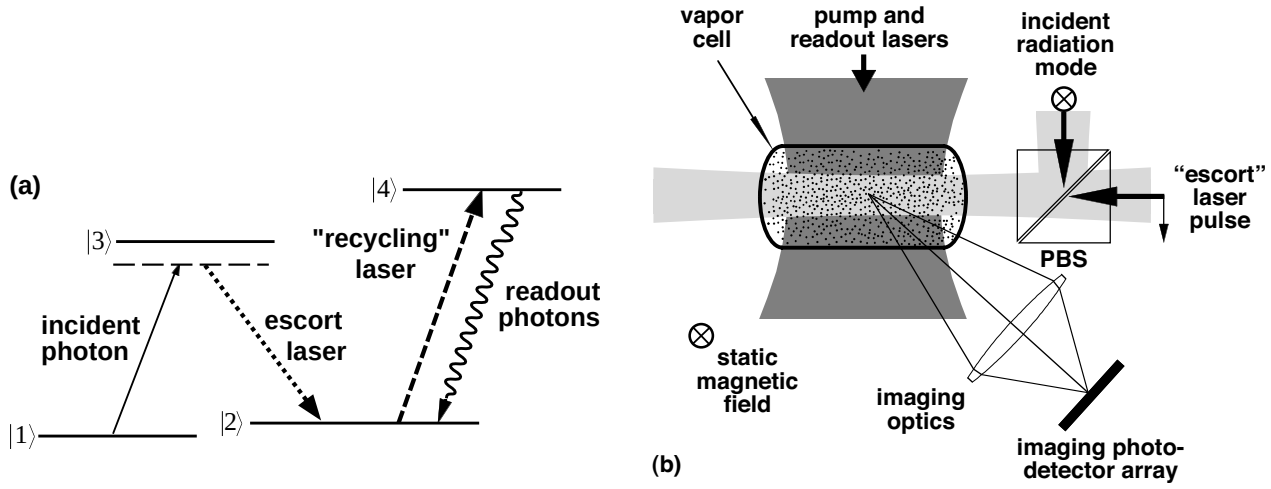

Figure 6. Simplified schematic showing atomic vapor scheme for achieving near unit-efficiency photon counting detection. (a) The relevant energy levels of the atomic species, e.g., Cesium, allow the incident photon, in the presence of a strong escort beam (dotted arrow) to enable a two-photon off-resonant (to level $|3\rangle$) Raman transition from the ground state $|1\rangle$ to the metastable state $|2\rangle$; the subsequent activation by the recycling pulse (dashed arrow) produces many photons from the repeated $|4\rangle \rightarrow |2\rangle$ transitions. (b) The experimental setup indicates how an imaging system might be used to count the number of excited atoms, and consequently the number of incident photons in the signal.

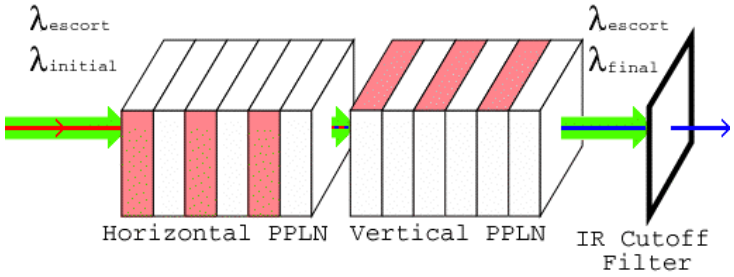

Figure 7. Simplified schematic showing system for quantum state transduction of an arbitrary input polarization state. Two perpendicularly oriented PPLN samples are used; the horizontal (vertical) polarization component of the input signal is up-converted in the first (second) crystal, by combining with the horizontal (vertical) component of the 1064-nm escort pulse. After correcting for some associated birefringent walkoff and phase shift effects, the polarization state of the incident signal should be faithfully converted to the higher frequency photon.

horizontal and vertical components. However, using the transformation methods described in Sect. 2.3, the final polarization state may be converted to match the input.

4.2. Quantum memory

There are a number of quantum information processing applications where a quantum memory for photons is required. These include: linear optics scalable quantum computing,[6, 32] quantum repeaters[2, 48] for long distance teleportation and quantum key distribution, and, as discussed in a companion article in these Proceedings,[49] cryptography protocols that involve special relativity in addition to quantum mechanics. Specifically, it is necessary to store the *state* of a photon, which in principle could be done by transferring the quantum information to a more permanent object, such as an atom. However, such systems for "stopped light" are not yet technologically possible at the single-photon level, or for durations more than ∼1 ms.[50, 51] Therefore, we are taking a more

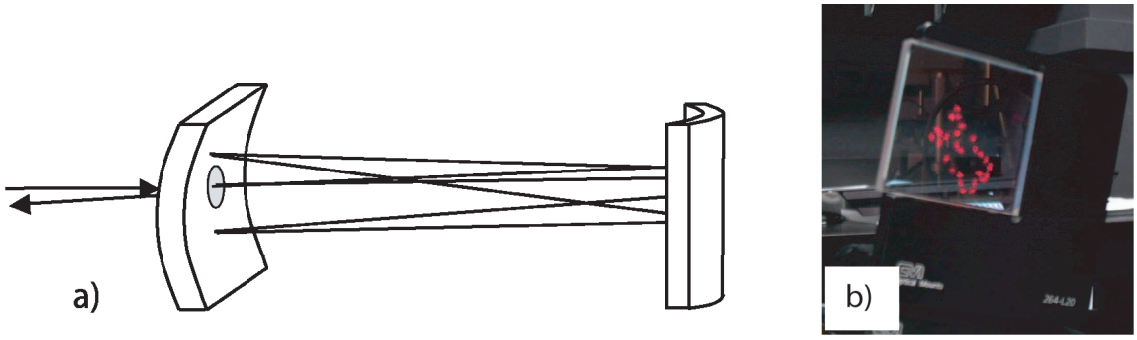

Figure 8. Low-loss optical storage system. (a) Using a pair of cylindrical mirrors (whose axes are nearly orthogonal), it is possible to realize a many-pass optical delay line with high transmission. In our current design, the photon enters via a small hole in one of the mirrors, and makes ~ 80 passes before leaving via the same hole. For a 2-meter long cavity, this implies a delay time of nearly 1 μs. High-reflectivity custom mirror coatings should enable transmissions in excess of 98%. (b) The spot pattern for a 50-pass system, observed via the small fraction of light scattering off one of the end mirrors.

direct approach, that of an ultralow-loss optical delay line (see Fig. 8). In contrast to the scheme of Pittman and Franson,[52] our delay line is similar to Herriott cells used in long path-length spectroscopy.[53] Two high-reflectivity mirrors are separated by approximately 2 m; one of them has a small aperture through which the light enters and, after a specified number of passes through the delay line, exits. Traditionally such delay lines have employed astigmatic mirrors, so that the resulting spot pattern on the mirrors fills much of the area (not possible with spherical mirrors), thus minimizing the leakage of light through the coupling hole before the desired exit cycle. Unfortunately, these mirrors are difficult to fabricate to the exacting standards we require. Instead, we have designed a system using a pair of cylindrical mirrors oriented at approximately right angles (see Fig. 8), but twisted slightly in order to introduce an effective astigmatism (for more details, see the accompanying article[49]). We have constructed a preliminary prototype of the system, and have been able to store light for nearly 1 μs.

The transmission with our present system is less than 20%, as the mirrors are not specifically coated for the optical wavelength we are using (670 nm). In fact, with 80 passes (159 reflections), the reflection probability per bounce is 98.9%. With readily obtainable mirror reflectivities over 99.99%, a transmission in excess of 98% is expected. It is also desirable that the delay line preserve the polarization of the stored photon **. Because all the incidence angles in our system are very close to normal, there is nothing to distinguish, e.g., horizontal and vertical polarization, so the system as a whole is expected to be essentially polarization insensitive. Preliminary measurements on our prototype storage cavity support this claim.

One potentially useful feature of such a storage system, if properly designed, is that the condition for a "re-entrant ray" (one which will exit via the entrance hole after a given number of passes) holds for *all* incident rays, as long as they do not at some point miss one of the mirrors. Such a feature is crucial for successful operation in a practical system, where one cannot necessarily guarantee the precise direction of the captured photons. Moreover, it means that our delay line could be used for simultaneous storage of multiple photons, or of a single photon for multiples of the base cavity storage time. Hence, it may be possible to use an extension of the system outlined here to store quantum states for up to 10 μs, with less than 2% loss (assuming mirror reflectivities of at least 99.999%, which is still an order of magnitude less than current state of the art).

**The more correct statement is that the storage system should at most apply some constant unitary transformation to the polarization, which could then be undone using a pair of waveplates after the cavity. However, if the delay line introduces decoherence to the state (as is perhaps more likely, e.g., in a fiber optic delay line), then compensation becomes difficult if not impossible.

ACKNOWLEDGMENTS

This research was funded by the DCI Postdoctoral Research Fellowship Program, ARDA, and the National Science Foundation (Grant #EIA-0121568). We would also like to acknowledge future support from a MURI Research Instrumentation grant, starting in 2003, to further develop these and other technologies.

REFERENCES

1. M. Nielsen and I. Chuang, *Quantum Computation and Quantum Information*, Cambridge University Press, 2000.
2. N. Gisin, G. Ribordy, W. Tittel, and H. Zbinden, "Quantum cryptography", *Rev. Mod. Phys.* **74**, pp. 145–195, 2002.
3. A. N. Boto, et al., "Quantum interferometric optical lithography: Exploiting entanglement to beat the diffraction limit", *Phys. Rev. Lett.* **85**, pp. 2733-2736, 2000; M. D'Angelo, M. V. Chekhova, and Y. Shih, "Two-photon diffraction and quantum lithography", *Phys. Rev. Lett.* **87**, pp. 012602, 2001.
4. R. Jozsa, Daniel S. Abrams, J. P. Dowling, and C. P. Williams, "Quantum clock synchronization based on shared prior entanglement", *Phys. Rev. Lett.* **85**, pp. 2010–2013, 2000; V. Giovannetti, S. Lloyd and L. Maccone, "Quantum-enhanced positioning and clock synchronization", *Nature* **412**, pp. 417–419, 2001; V. Giovannetti, S. Lloyd, L. Maccone, and F. N. C. Wong, "Clock synchronization with dispersion cancellation", *Phys. Rev. Lett.* **87**, pp. 117902, 2001.
5. D. Bouwmeester, A. Ekert, and A. Zeilinger (eds.), *The Physics of Quantum Information*, Springer, 2000.
6. E. Knill, R. LaFlamme and G. J. Milburn, "A scheme for efficient quantum computation with linear optics", *Nature* **409**, pp. 46–52, 2001.
7. P. G. Kwiat, "Hyper-Entangled States", *J. Mod. Opt.* **44**, pp. 2173–2178, 1997.
8. P. G. Kwiat, et al., "New high-intensity source of polarization-entangled photon pairs", *Phys. Rev. Lett.* **75**, pp. 4337–4340, 1995.
9. P. G. Kwiat, E. Waks, A. G. White, I. Appelbaum, and P. H. Eberhard, "Ultrabright source of polarization-entangled photons," *Phys. Rev. A.* **60**, pp. R773–776, 1999.
10. P. Michler, et al., "A quantum dot single-photon turnstile device", *Science* **290**, pp. 2282–2285, 2000; C. Santori, et al., "Triggered single photons from a quantum dot", *Phys. Rev. Lett.* **86**, pp. 1502–1505, 2001; E. Moreau, et al., "Single-mode solid-state single-photon source based on isolated single quantum dots in pillar microcavities", *Appl. Phys. Lett.* **79**, pp. 2865–2867, 2001; C. Santori, et al., "Indistinguishable photons from a single-photon device", *Nature* bf 419, pp. 594–597, 2002.
11. C. Kurtsiefer, S. Mayer, P. Zarda, and H. Weinfurter, "A stable solid-state source of single photons", *Phys. Rev. Lett.* **85**, pp. 290–293, 2000; R. Brouri, A. Beveratos, J.-P. Poizat, and P. Grangier, "Photon antibunching in the fluoresecence of individual colored centers", *Opt. Lett.* **25**, pp. 1294–1296, 2000.
12. A. Kuhn, M. Hennrich, and G. Rempe, "Deterministic single-photon source for distributed quantum networking," *Phys. Rev. Lett.* **89**, pp. 067901, 2002.
13. C. K. Hong and L. Mandel, "Experimental realization of a localized one-photon state", *Phys. Rev. Lett.* **56**, pp. 58–60, 1986.
14. T. Aichele, A. I. Lvovsky and S. Schiller, "Optical mode characterization of single photons prepared by means of conditional measurements on a biphoton state", *Eur. Phys. J. D* **18**, pp. 237–245, 2002.
15. T. B. Pittman, B. C. Jacobs, and J. D. Franson,"Single photons on pseudodemand from stored parametric down-conversion", *Phys. Rev. A* **66**, pp. 042303, 2002; A. L. Migdall, D. Branning, and S. Castelletto,"Tailoring single-photon and multiphoton probabilities of a single-photon on-demand source", *Phys. Rev. A* **66**, pp. 053805, 2002.
16. L. E. Myers, et al., "Quasi-phase-matched optical parametric oscillators in bulk periodically poled LiNbO3", *J. Opt. Soc. Am. B*, **12**, pp. 2102–2116, 1995; L. E. Myers and W. R. Bosenberg, "Periodically poled lithium niobate and quasi-phase-matched optical parametric oscillators", *IEEE J. Quant. Elect.* **33**, pp. 1663–1672, 1997; L. Chanvillard, et al., "Soft proton exchange on periodically poled LiNbO3: A simple waveguide fabrication process for highly efficient nonlinear interactions", *App. Phys. Lett.* **76**, pp. 1089–1091, 2000.

17. S. Tanzilli, et al., "Highly efficient photon-pair source using a Periodically Poled Lithium Niobate waveguide", *Elect. Lett.* **37**, pp. 26–28, 2001; K. Kawahara, and T. Kuga, "New high-efficiency source of photon pairs for engineering quantum entanglement", *Phys. Rev. Lett.* **86**, pp. 5620–5623, 2001; S. Tanzilli, et al., "PPLN waveguide for quantum communication", *Eur. Phys. J. D* **18**, pp. 155–160, 2002.
18. J. Kim, S. Takeuchi, Y. Yamamoto, and H. H. Hogue, "Multiphoton detection using visible light photon counter", *Appl. Phys. Lett.* **74**, pp. 902–904, 1999; S. Takeuchi, J. Kim, Y. Yamamoto, and H. Hogue, "Development of a high-quantum-efficiency single-photon counting system", *ibid.* **74**, pp. 1063–1065, 1999.
19. K. Banaszek and I. A. Walmsley, "Photon counting with a loop detector", *Opt. Lett.* **28**, pp. 52-54, 2003; K. Nemoto and S. L. Braunstein, "Equivalent efficiency of a simulated photon-number detector", *Phys. Rev. A* **66**, pp. 032306, 2002; J. Rehacek, et al., "Multiple-photon resolving fiber-loop detector" *Phys. Rev. A* **67**, pp. 061801(R), 2003.
20. M. Pelton, et al., "Bright, single-mode source of frequency non-degenerate, polarization-entangled photon pairs using periodically poled KTP", *Conference on Lasers and Electrooptics/Quantum Electronics and Laser Science*, postdeadline presentation, 2003.
21. A. J. Berglund, *Quantum coherence and control in one- and two-photon optical systems*, Dartmouth College B.A. Thesis, 2000; also quant-ph/0010001.
22. R. Jozsa, "Fidelity for Mixed Quantum States", *J. Mod. Opt.* **41**, pp. 2315-2324, 1994.
23. N. Peters, et al., "Precise Creation, Characterization, and Manipulation of Single Optical Qubits", submitted to a Special Issue in *J. Mod. Opt.*, 2003.
24. A. G. White, D. F. V. James, P. H. Eberhard, and P. G. Kwiat, "Non-maximally entangled states: Production, characterization, and utilization", *Phys. Rev. Lett.* **83**, pp. 3103–3106, 1999.
25. G. M. Palma, K. A. Suominen, A. K. Ekert, "Quantum computers and dissipation", *Proc. R. Soc. London A* **452**, pp. 567–584, 1996; L. M. Duan, G. C. Guo, "Preserving coherence in quantum computation by pairing quantum bits", *Phys. Rev. Lett.* **79**, pp. 1953–1956, 1997; P. Zanardi, M. Rasetti, "Noiseless quantum codes", *Phys. Rev. Lett.* **79**, pp. 3306–3309, 1997; D. A. Lidar, I. L. Chuang, K. B. Whaley,"Decoherence-free subspaces for quantum computation", *Phys. Rev. Lett.* **81**, pp. 2594-2597, 1998.
26. P. G. Kwiat, A. J. Berglund, J. B. Altepeter, and A. G. White, "Experimental verification of decoherence-free subspaces", *Science* **290**, pp. 498–500, 2000; J. B. Altepeter, et al., "Experimental investigation of a two-qubit decoherence-free subspace", submitted to *Phys. Rev. Lett.*, 2003.
27. A. G. White, D. F. V. James, W. J. Munro, and P. G. Kwiat, "Exploring Hilbert space: Accurate characterization of quantum information", *Phys. Rev. A* **65**, pp. 012301, 2002.
28. J. B. Altepeter, et al., "Ancilla-assisted quantum process tomography", *Phys. Rev. Lett.* **90**, pp. 193601, 2003.
29. J. B. Altepeter, D. James, P. G. Kwiat, W. Munro, N. Peters, and T. C. Wei, in preparation.
30. D. F. V. James, P. G. Kwiat, W. J. Munro, and A. G. White, "Measurement of qubits", *Phys. Rev. A* **64**, pp. 052312, 2001.
31. W. J. Munro, D. F. V. James, A. G. White, and P. G. Kwiat, "Maximizing the entanglement of two mixed qubits", *Phys. Rev. A* **64**, pp. 030302, 2001; T.-C. Wei, et al., "Maximal entanglement versus entropy for mixed quantum states", *Phys. Rev. A* **67**, pp. 022110, 2003.
32. S. Glancy, J. M. LoSecco, H. M. Vasconcelos and C. E. Tanner, "Imperfect detectors in linear optical quantum computers", *Phys. Rev. A* **65**, pp. 062317, 2002; S. D. Bartlett, E. Diamanti, B. C. Sanders, and Y. Yamamoto, "Photon counting schemes and performance of non-deterministic nonlinear gates in linear optics", *Free-Space Laser Communication and Laser Imaging II*, J. C. Ricklin and D. G. Voelz, eds., *Proc. SPIE* **4821**, 2002; also in quant-ph/0204073.
33. P. Kok and S. L. Braunstein, "Detection devices in entanglement-based optical state preparation", *Phys. Rev. A* **63**, pp. 033812, 2001; H. Lee, P. Kok, N. J. Cerf, and J. P. Dowling, "Linear optics and projective measurements alone suffice to create large-photon-number path entanglement", *Phys. Rev. A* **65**, pp. 030101(R), 2002.
34. R. J. Hughes, G. L. Morgan, and C. G. Peterson, "Quantum key distribution over a 48-km optical fiber network", *J. Mod. Opt.* **47**, pp. 533–540, 2000.
35. P. G. Kwiat, et al., "High efficiency single-photon detectors", *Phys. Rev. A* **48**, R867–R870, 1993.

36. D. Stucki, et al., "Photon counting for quantum key distribution with Peltier cooled InGaAs/InP APDs", *J. Mod. Opt.* **48** pp. 1967–1981, 2001; M. Bourennane, A. Karlsson, J. P. Ciscar, and M. Mathes, "Single-photon counters in the telecom wavelength region of 1550 nm for quantum information processing", *J. Mod. Opt.* **48**, pp. 1983–1995, 2001.
37. B. Cabrera, et al., "Detection of single infrared, optical, and ultraviolet photons using superconducting transitino edge sensors", *Appl. Phys. Lett.* **73**, pp. 735–737, 1998; G. Di Giuseppe, et al., "Observation of bosonic coalescence of photon pairs", quant-ph/0306131.
38. A. Verevkin, et al., "Detection efficiency of large-active-area NbN single-photon superconducting detectors in the ultraviolet to near-infrared range", *Appl. Phys. Lett.* **80**, pp. 4687–4689, 2002.
39. A. P. VanDevender and P. G. Kwiat, "High efficiency single photon detection via frequency up-conversion", submitted to J. Mod. Opt., 2003.
40. L. E. Myers, et al., "Quasi-phase matched optical parametric oscillators in bulk periodically poled LiNbO3", *J. Opt. Soc. Am. B* **12**, pp. 2102–2116, 1995.
41. M. A. Albota and F. N. C. Wong, "Efficient single-photon counting at 1.55 μm via frequency upconversion", in Postdeadline Papers Book, *Conf. on Lasers and Electro-Optics/Quantum Electronics & Laser Science Conference* (CLEO/QELS), 2003.
42. D. F. V. James and P. G. Kwiat, "Atomic vapor-based high efficiency optical detectors with photon number resolution", *Phys. Rev. Lett.* **89**, pp. 183601, 2002.
43. A. Imamoglu, "High efficiency photon counting using stored light", *Phys. Rev. Lett.* **89**, pp. 163602, 2002.
44. M. A. Rowe, et al.,"Experimental violation of a Bell's inequality with efficient detection", *Nature* **409**, pp. 791–794, 2001.
45. D. F. V. James and P. G. Kwiat, in preparation, 2003.
46. S. Lloyd, M.S. Shahriar, J.H. Shapiro, and P.R. Hemmer, "Long distance, unconditional teleportation of atomic states via complete Bell state measurements", *Phys. Rev. Lett.* **87**, pp. 167903, 2001.
47. Y. H. Kim, S. P. Kulik, and Y. Shih, "Quantum teleportation of a polarization state with a complete Bell state measurement", *Phys. Rev. Lett.* **86**, pp. 1370–1373, 2001.
48. M. Zukowski, A. Zeilinger, M. A. Horne, and A. Ekert, "'Event-ready-detectors' Bell experiment via entanglement swapping", *Phys. Rev. Lett.* **71**, pp. 4287–4290, 1993; H.-J. Briegel, W. Duer, J.-I. Cirac, and P. Zoller, "Quantum repeaters: The role of imperfect local operations in quantum communication", *Phys. Rev. Lett.* **81**, pp. 5932–5945, 1998.
49. E. Jeffrey and P. Kwiat, "Delayed-choice quantum cryptography", in *Quantum Communications and Quantum Imaging Conferences*, R. E. Meyers and Y. Shih, eds., *Proc. SPIE* **5161**, 2003.
50. M. D. Lukin and A. Imamoglu,"Controlling photons using electromagnetically induced transparency", *Nature* **413**, pp. 273–275, 2001.
51. A. E. Kozhekin, K. Molmer, and E. Polzik, "Quantum memory for light", *Phys. Rev. A* **62**, pp. 033809, 2000.
52. T. B. Pittman and J. D. Franson, "Cyclical quantum memory for photonic qubits," *Phys. Rev. A* **66**, pp. 062302, 2002.
53. D. R. Herriott and H. J. Schulte, "Folded optical delay lines", *Appl. Opt.* **4**, pp. 883–885, 1965.